Interstellar Matter and Star Formation:
A Multi-wavelength Perspective
ASI Conference Series, 2010, Vol. 1, pp 91–97
Edited by D.K. Ojha

AKARI far-infrared observations of the ISM in nearby galaxies

H. Kaneda[1*], T. Suzuki[2], M. Yamagishi[1], T. Onaka[3],
D. Ishihara[1], I. Sakon[3], T. Shimonishi[3] and I. Takase[3]
[1] *Graduate School of Science, Nagoya University, Nagoya 464-8602, Japan*
[2] *Advanced Technology Center, National Astronomical Observatory of Japan, Tokyo 181-8588, Japan*
[3] *Graduate School of Science, The University of Tokyo, Bunkyo-ku, Tokyo 113-0033, Japan*

Abstract. Far-infrared (FIR) properties of 57 nearby galaxies are studied using the Far-Infrared Surveyor (FIS) on AKARI. Among them, this paper focuses on the results obtained for the three famous nearby edge-on galaxies, NGC 3079, M82, and NGC253, which show prominent galactic superwinds in the X-ray and Hα. These galaxies exhibit very bright nuclei in the FIR due to starburst activity. We have spatially resolved the central regions of these galaxies, among which we have detected FIR dust emission in the haloes of M 82 and NGC 253. We discuss similarities and differences in the FIR properties among the three galaxies.

Keywords : galaxies: halos — galaxies: individual(M 82, NGC 253, NGC 3079) —galaxies: starburst — infrared: galaxies — ISM: dust, extinction

1. Introduction

AKARI is the first Japanese satellite dedicated to infrared astronomy, launched on February 21 (UT), 2006 (Murakami et al. 2007). AKARI carries on board two scientific instruments, the Far-Infrared Surveyor (FIS; Kawada et al. 2007) and the Infrared Camera (IRC; Onaka et al. 2007), which cover the wavelength

*e-mail: kaneda@u.phys.nagoya-u.ac.jp

ranges of ∼50–180 μm and ∼2–27 μm, respectively. With AKARI, we have performed near- to far-infrared (NIR–FIR) imaging and spectroscopic observations of the ISM in our Galaxy and nearby galaxies as one of the AKARI mission programs called ISMGN (ISM in our Galaxy and Nearby galaxies; Kaneda et al. 2009a). We introduce here, our FIR observations of nearby galaxies. In total, 57 galaxies are studied using the FIS. They have been observed relatively deeply in a pointing mode, not during the All-Sky Survey that is the primary observation mode of AKARI, and therefore galaxies with high visibility to AKARI (i.e. high ecliptic latitudes) have been preferentially selected.

The AKARI/FIS has 4 photometric bands in the FIR; 2 wide bands at the central wavelengths of 90 and 140 μm ($WIDE-S$ and $WIDE-L$)and 2 narrow bands at 65 μm and 160 μm ($N60$ and $N160$). The wide bands provide high sensitivities, while the 2 narrow bands combined with the 2 wide bands are useful to accurately determine the temperatures of the FIR dust. Besides the fine allocation of the photometric bands, the special fast reset mode of the FIS provides high signal saturation levels, therefore we can safely observe very bright sources without serious saturation effects. Hence, the uniqueness of the FIS as compared to any other previous or currently existing instruments is a combination of its high saturation limits and high sensitivity (i.e. large dynamic ranges of signal detection) with relatively high spatial resolution.

We focus here on the results obtained for the three famous edge-on nearby galaxies, NGC 3079, M 82, and NGC 253, which show prominent galactic superwinds in the X-ray and Hα. The galactic center of each galaxy shows nuclear starburst activity. Their inclination angles are similar to each other, as large as about 80°. Hence, they are interesting targets for the study of the vertical distribution of dust grains as well as the dust properties in their super-winds and galactic halos. Thanks to the large dynamic ranges of signal detection with the FIS, we have spatially resolved the central regions of these galaxies, among which we have firmly detected FIR dust emission in the haloes of M82 and NGC253. We discuss similarities and differences in the FIR properties among the three galaxies.

2. Observations

We performed FIR observations of NGC 3079 in April of 2007, M 82 in April and October of 2006, and NGC 253 in June of 2007 in a slow scan mode of the FIS (Shirahata et al. 2009). The FIR images were processed from the FIS Time Series Data (TSD) using the AKARI official pipeline. At the time of writing of this paper, the 2 narrow bands still suffer ghost image problems originating from the very bright centers (Kawada et al. 2007), which cause considerable uncertainties in the fluxes from the center and halo regions. Thus we concentrate below on the 2 wide bands. We adopt the distances of 15.6 Mpc

(Sofue & Irwin 1992), 3.6 Mpc (Freedman et al. 1994), and 3.5 Mpc (Rekola et al. 2005) to NGC 3079, M 82, and NGC 253, respectively.

3. Results

Fig. 1 shows the FIR images of NGC 3079 obtained with the FIS, together with the NIR and MIR images with the IRC for demonstration purposes. These are the complete dataset of one galaxy in our sample. The structure of the galaxy is different from band to band. In the NIR, emission from evolved stars is prominent along the bar, while in the MIR, the center and the arm regions are bright, among which relative intensities are different. The MIR emission is attributed mostly to polycyclic aromatic hydrocarbons (PAHs) in the 7 and 11 μm bands (Weedman et al. 2005) and hot dust emission in the other bands. In the FIR images, cold dust emission from the galaxy is largely extended along the edge-on disk, but not significantly along the minor axis. The 24 μm image shows extended emission in the center, significantly broader than the point spread function (PSF) of $\sim 5''$ in FWHM (Onaka et al. 2007). Hence, the central extended emission can be associated with the galactic superwinds (Yamagishi et al., in prep.).

Here and hereafter, we define the center region as a circular area within a radius of 2 kpc at the galactic center, which corresponds to angular diameters of $\sim 1'$ for NGC 3079 and $\sim 4'$ for M 82 and NGC 253. We derive the flux

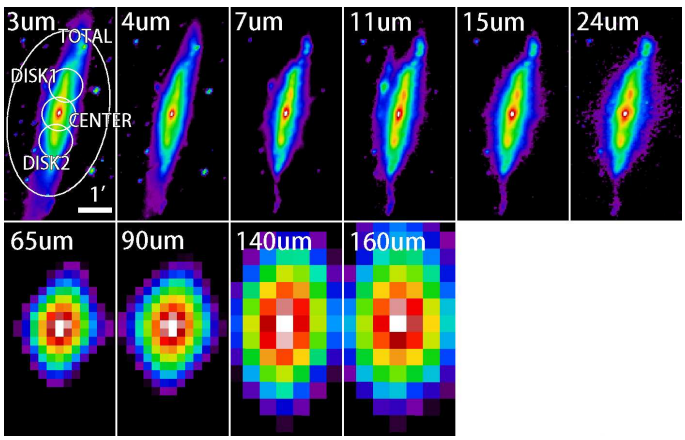

Figure 1. Datasets of an AKARI sample nearby galaxy: the 3 μm, 4 μm, 7 μm, 11 μm, 15 μm, 24 μm, 65 μm, 90 μm, 140 μm, and 160 μm images of the edge-on spiral galaxy NGC 3079. North is up and east is to the left. The color levels are set in a log scale where the lowest levels are 0.1 % (3–24 μm bands) and 5 % (65–160 μm bands) of the peak surface brightness.

densities of the center region in NGC 3079 by integrating the surface brightness within the circular aperture in the $WIDE-S$ (90 μm) and $WIDE-L$ (140 μm) bands. Since the aperture size is not sufficiently large as compared to the PSF sizes of the FIS ($\sim 30''$; Kawada et al. 2007), we consider aperture corrections (Shirahata et al. 2009). We also obtain the flux densities from the whole galaxy by integrating the surface brightness within a diameter of $5'$. The values thus obtained are listed in Table 1 (F_{90} and F_{140}), where the flux uncertainties including both systematic effects associated with the FIR detectors and absolute calibration uncertainties are estimated to be no more than 20 % for $WIDE-S$, and 30 % for $WIDE-L$ (Kawada et al. 2007). From the ratios of the $WIDE-S$ to the $WIDE-L$ flux density, we estimate the temperatures of FIR dust, $T_{\rm dust}$, to be 33 K for the center and 31 K for the total region, using the emissivity power-law index of $\beta = 1$. We then calculate dust mass by using the equation (e.g. Hildebrand 1983):

$$M_{\rm dust} = \frac{4a\rho D^2}{3} \frac{F_\nu}{Q_\nu B_\nu(T)}, \quad (1)$$

where $M_{\rm dust}$, D, a, and ρ are the dust mass, the galaxy distance, the average grain radius, and the specific dust mass density, respectively. F_ν, Q_ν, and $B_\nu(T)$ are the observed flux density, the grain emissivity, and the value of the Planck function at the frequency of ν and the dust temperature of T. We adopt the grain emissivity factor given by Hildebrand (1983), the average grain radius of 0.1 μm, and the specific dust mass density of 3 gm cm^{-3}. We use the 90 μm flux densities from Table 1 and the above dust temperatures. The dust mass thus derived is listed in Table 1.

Figures 2 and 3 show the FIR images of M 82 and NGC 253, respectively. We detect faint extended dust emission in the haloes of M 82 and NGC 253 up to 8 kpc and 9 kpc beyond the disk, respectively, both of which show spatial coincidence with the X-ray plasma outflows (Kaneda et al. 2009b; Kaneda et al. in prep.). Thus, the extended FIR emissions are likely to represent outflowing dust entrained by galactic superwinds. The circular apertures used to obtain the flux densities in the center region as well as the halo regions are shown in each image, where the diameter of each aperture is $4'$ ($\simeq$ 4 kpc). To obtain the total flux densities from the whole galaxies, we adopt the largest circular apertures in both $WIDE-S$ and $WIDE-L$ images, which are $12'.5$ and $11'.5$ in diameter for M 82 and NGC 253, respectively.

The dust temperatures and masses in the center, halo, and total regions of M 82 and NGC 253 are obtained in the same manner as described above. The values thus obtained for the three galaxies are summarized in Table 1. The gas masses in Table 1 are obtained from literature and from published HI/CO maps (Koda et al. 2002; Devereux & Young 1990; Radovich et al. 2001; Houghton et al. 1997; Walter et al. 2002; Yun et al. 1994). The properties of the dust and their relation to the gas are considerably different from galaxy

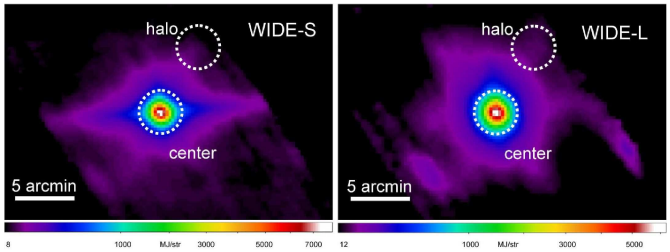

Figure 2. FIR images of M 82 obtained with the AKARI/FIS in the $WIDE-S$ (90 μm) and $WIDE-L$ (140 μm) bands. North is up and east is to the left. The color levels are stretched to very low levels: 0.1 % and 0.2 % of the peak surface brightness for the $WIDE-S$ and $WIDE-L$, respectively. The elongation in the east-west direction seen in the $WIDE-S$ images is detector artifacts due to optical cross talk among the pixels of the monolithic arrays used for this band (Kawada et al. 2007).

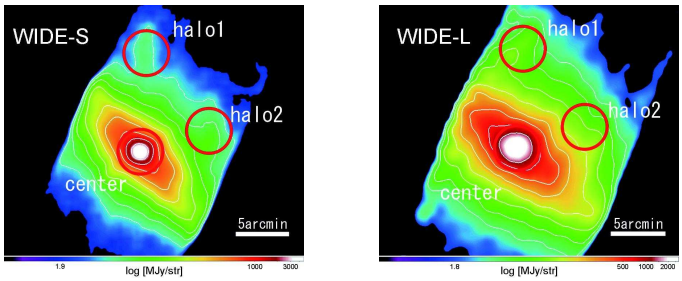

Figure 3. FIR images of NGC 253 obtained with the AKARI/FIS in the $WIDE-S$ (90 μm) and $WIDE-L$ (140 μm) bands. North is up and east is to the left. The contours are drawn at surface brightness levels of 10, 20, 40, 80, 160, 320, 640, 1280, and 2560 MJy/str (the last one is only for WIDE-S).

Table 1. Basic properties of FIR dust in the observed edge-on galaxies.

Target	Region	F_{90} Jy	F_{140} Jy	$T_{\rm dust}$ K	$M_{\rm dust}$ $M_\odot$	$M_{\rm gas}$ $M_\odot$	$M_{\rm gas}/M_{\rm dust}$
NGC 3079	total	103	120	31	1.4×10^7	1.2×10^{10}	860
	center	54	53	33	5.6×10^6	5×10^9	900
M 82	total	2200	2120	34	1.1×10^7	2.1×10^9	200
	center	1670	1500	37	5.5×10^6	1.5×10^9	300
	halo	16	26	23	5×10^5	4×10^6	10
NGC 253	total	1940	2370	28	2.4×10^7	2.4×10^9	100
	center	1200	1300	31	8.3×10^6	1.3×10^9	150
	halo1&2	28	64	20	2×10^6	8×10^7	40

to galaxy. From the temperature of dust, nuclear starburst activity is likely highest in M 82, while the amount of dust is largest in NGC 253. The gas mass is by far largest for NGC 3079, giving unusually high gas-to-dust mass ratios in the center and even the total region of the galaxy. The dust mass is most centrally-concentrated in M 82, while it is rather distributed in NGC 253. The dust in the halo is most abundant in NGC 253. In contrast, we do not detect dust emission extended in the halo of NGC 3079, although it is expected to have an observable extension of $\sim 2'$ from the center along the minor axis by assuming physical elongation ($8 - 9$ kpc) similar to M 82 and NGC 253. We suggest that these differences reflect different evolutionary stages of nuclear starburst activity among the three galaxies; NGC 3079 seems to be at the earliest stage, while NGC 253 is at the last stage. On the other hand, the gas-to-dust mass ratio has a common tendency to decrease from the inner to the outer regions, implying that the metal-enriched gas injected by the nuclear starburst significantly contributes to the total mass of wind material.

4. Summary

Among the 57 nearby galaxies observed in the FIR with AKARI, we have presented the results for the three famous nearby edge-on galaxies, NGC 3079, M82, and NGC253, which show prominent galactic superwinds in the X-ray and Hα. We detect FIR dust emission in the haloes of M82 and NGC253. We obtain the temperatures and masses of dust as well as gas-to-dust mass ratios in the inner 4 kpc area and the halo regions as well as the whole galaxy for each target. From the differences in the FIR properties found among the three galaxies, we suggest that they are at different evolutionary stages of nuclear starburst activity.

Acknowledgements

We thank all the members of the AKARI projects, particularly those belonging to the ISMGN working group. AKARI is a JAXA project with the participation of ESA.

References

Freedman W. L., Hughes S. M., Madore B. F., et al., 1994, ApJ, 427, 628
Devereux N. A., & Young J. S., 1990 ApJ, 359, 42
Kaneda H., Koo B.-C., Onaka T., & Takahashi H., 2009a, Adv.Sp.Res., 44, 1038
Kaneda H., Yamagishi M., Suzuki T., & Onaka T., 2009b, ApJ, 698, L125
Kawada M., Baba H., Barthel P. D., et al., 2007, PASJ, 59, 389
Koda J., Sofue Y., Kohno K., et al., 2002, ApJ, 573, 105
Hildebrand R. H., 1983, QJRAS, 24, 267

Houghton S., Whiteoak J. B., Koribalski B., et al., 1997, A&A, 325, 923
Murakami H., Baba H., Barthel P., et al., 2007, PASJ, 59, 369
Onaka T., Matsuhara H., Wada T., et al., 2007, PASJ, 59, 401
Radovich M., Kahanpää J., & Lemke D., 2001, A&A, 377, 73
Rekola R., Richer M. G., McCall M. L., et al., 2005, MNRAS, 361, 330
Shirahata M., Matsuura S., Hasegawa S., et al., 2009, PASJ, 61, 737
Sofue Y., & Irwin J. A., 1992, PASJ, 44, 353
Walter F., Weiss A., & Scoville N., 2002, A&A, 580, L21
Weedman D. W., Hao L., Higdon S. J. U., et al., 2005, A&A, 633, 706
Yun M. S., Ho P. T. P., & Lo K. Y., 1994, Nature, 372, 530